Temporary upregulation of anti-inflammatory cytokine IL-13 expression in the brains of CD14 deficient mice in the early stage of prion infection

CrossMark

Rie Hasebe, Akio Suzuki, Takeshi Yamasaki, Motohiro Horiuchi *

Laboratory of Veterinary Hygiene, Graduate School of Veterinary Medicine, Hokkaido University, Nishi 9, Kita 18, Kita-ku, Sapporo 060-0818, Japan

ARTICLE INFO

ABSTRACT

CD14 deficient (CD14$^{-/-}$) mice survived longer than wild-type (WT) C57BL/6J mice when inoculated with prions intracerebrally, accompanied by increased expression of anti-inflammatory cytokine IL-10 by microglia in the early stage of infection. To assess the immune regulatory effects of CD14 in detail, we compared the gene expression of pro- and anti-inflammatory cytokines in the brains of WT and CD14$^{-/-}$ mice infected with the Chandler strain. Gene expression of the anti-inflammatory cytokine *IL-13* in prion-infected CD14$^{-/-}$ mice was temporarily upregulated at 75 dpi, whereas *IL-13* gene expression was not upregulated in prion-infected WT mice. Immunofluorescence staining showed that IL-13 was mainly expressed in neurons of the thalamus at 75 dpi. These results suggest that CD14 can suppress IL-13 expression in neurons during the early stage of prion infection.

© 2014 Elsevier Inc. All rights reserved.

1. Introduction

Prion diseases are fatal neurodegenerative disorders including scrapie in sheep and goats, bovine spongiform encephalopathy in cattle, chronic wasting disease in cervids, and Creutzfeldt–Jakob disease in humans. These diseases are characterized in the central nervous system (CNS) by deposition of the disease-specific form of prion protein (PrP^{Sc}), vacuolation of neurons and neuropil, astrocytosis and microglial activation. Despite little recruitment of adaptive immune cells into the CNS in prion diseases, innate immunity is reported to be involved in the pathogenesis of prion diseases [1].

CD14 is expressed by monocytes and macrophages as a glycosylphosphatidylinositol-anchored membrane form and a soluble form [2,3]. The binding of pathogen-associated molecular patterns to CD14 clusters transmembrane proteins including toll-like receptors (TLR) 2 and 4 to induce gene expression of pro-inflammatory mediators [4,5]. We recently showed that CD14 has a progressive role in the neuropathogenesis of prion diseases [6]. CD14 knockout (CD14$^{-/-}$) mice survived longer than wild-type (WT) mice after intracerebral inoculation with prions, with reduced deposition of PrP^{Sc} and prion infectivity in the early to middle stage of the infection. Our data showed that expression of an anti-inflammatory cytokine IL-10 was increased in brains of CD14$^{-/-}$ mice in the early stage of prion infection, accompanied by accelerated microglial

activation. This suggests that CD14 has suppressive roles in anti-inflammatory responses and microglial activation in prion-infected mouse brain. Further analyses of influence of CD14-deficiency on the inflammatory condition in prion-infected mouse brains could provide valuable information regarding the immune regulatory effects by CD14 molecule. Thus, we compared the gene expression profiles of pro- and anti-inflammatory cytokines in prion-infected WT and CD14$^{-/-}$ mice.

2. Materials and methods

2.1. Mice

Six-week-old female C57BL/6J WT mice (Japan Clea Inc.) and CD14$^{-/-}$ congenic mice B6.129S-Cd14$^{<tm1Frm>}$/J (Jackson Laboratories) were inoculated intracerebrally with 2.5% brain homogenates from scrapie Chandler strain-infected WT mice or from age-matched uninfected WT mice for a negative control. All animal procedures were approved by the Institutional Animal Care and Use Committee of the Graduate School of Veterinary Medicine, Hokkaido University.

2.2. Quantitative RT-PCR

The brains were sliced using the Alto™ Brain Matrix (Roboz Surgical Instrument Co.) at a thickness of 1 mm. The thalamus, hippocampus and combined regions of internal capsule (ic), fimbria of hippocampus (fi) and cerebral peduncle (cp) were dissected from

the slice around the bregma −1.82 mm [7] under a stereoscopic microscope. Total RNA was extracted using TRIZOL® reagent (Thermo Scientific). Gene expression was analyzed by quantitative RT-PCR using the TaqMan Gene Expression Assay as described previously [6]. TaqMan Gene Expression Assays used here were IFN-γ (*ifng*, Mm99999056_m1), IL-1β (*il1β*, Mm01336189_m1), IL-6 (*il6*, Mm99999064_m1) and Nos2 (*nos2*, Mm01309902_m1) for pro-inflammatory cytokines, and IL-4 (*il4*, Mm00445259_m1), IL-13 (*il13*, Mm00434204_m1), IL-10 (*il10*, Mm99999062_m1), TGF-β (*tgfβ*, Mm03024053_m1) and IL-1 receptor antagonist (*il1ran*, Mm00446186_m1) for anti-inflammatory cytokine.

2.3. Immunofluorescence staining

For PrP^{Sc} specific staining, anti-mouse prion protein mouse monoclonal antibody (mAb) 132 was prepared as described previously [8]. Immunofluorescence staining for cytokines and neural markers was performed as described previously [6]. Dilutions of antibodies were 1:800 for CD68 (rat mAb, clone FA-11), 1:200 for CD11b (rat mAb, clone M1/70), NeuN (mouse mAb, clone A60), IL-13 (rabbit polyclonal Ab, Abcam, No. ab79277), and IL-13Rα1 (rabbit polyclonal Ab, Abcam, No. ab106732), 1:500 for GFAP (rat mAb, clone 2.2B10), 1:1000 for GFAP (rabbit polyclonal Ab, Dako, No. Z033401) and 1:2000 for all Alexa Fluor-labeled antibodies (Thermo Scientific).

3. Results

3.1. Gene expression of IL-13 is temporarily up-regulated in CD14$^{-/-}$ mice in the early stage of prion infection

Expression of an anti-inflammatory cytokine IL-10 was increased, whereas a pro-inflammatory cytokine IL-1β was decreased in certain areas of CD14$^{-/-}$ mouse brains in the early stage of prion infection, suggesting that inflammatory condition was shifted to anti-inflammatory status in the absence of CD14 [6]. Here we analyzed inflammatory condition in the brains more in detail by comparing gene expression of pro- and anti-inflammatory cytokines between WT and CD14$^{-/-}$ mice by quantitative RT-PCR. The thalamus, hippocampus, and the area combined with internal capsule, fimbria of hippocampus and cerebral peduncle were chosen, since difference in the microglial activation between WT and CD14$^{-/-}$ mice was prominent in these areas at 60 and 75 dpi (Fig. 1).

IL-13 gene expression at 75 dpi was higher in prion-infected CD14$^{-/-}$ mice than in prion-infected WT mice in all examined areas, and these differences were statistically significant for the thalamus and hippocampus (Fig. 2B and D). In the regions of ic, fi and cp, IL-13 gene expression was detected in 2 of 3 prion-infected-CD14$^{-/-}$ mice at 75 dpi (Fig. 2C). However, in prion-infected WT mice and mock-infected mice, IL-13 expression was below the detection limit (Fig. 2C). Interestingly, the temporarily upregulated IL-13 gene expression in CD14$^{-/-}$ mouse brains was restored to the steady-state level at 90 dpi and thereafter (Fig. 2B–D). In the hippocampus, gene expressions of pro-inflammatory cytokines were significantly higher in prion-infected WT mice than in prion-infected CD14$^{-/-}$ mice: IL-1β at 120 dpi and IL-6 at 90 dpi (Fig. 2D). Cytokine genes significantly upregulated by prion infection both in WT and CD14$^{-/-}$ mice were as follows: IL-1β at 75 and 120 dpi, IL-6 at 75 dpi, TGF-β at 75 dpi and IL1 receptor antagonist (IL1ran) at 75 and 120 dpi in the thalamus (Fig. 2B), and IL-6 at 75 dpi, IFN-γ at 75 dpi and TGF-β at 75 and 90 dpi in the hippocampus (Fig. 2D). The gene expressions of IL-4 and IL-10 were below the limit of detection in all samples (data not shown).

3.2. IL-13 expression is upregulated in neurons of the thalamus in CD14$^{-/-}$ mice only in the early stage of prion infection

To confirm the results of the gene expression analysis, we examined IL-13 expression by immunofluorescence staining (Fig. 3A). In prion-infected CD14$^{-/-}$ mice at 75 dpi, IL-13 was most frequently expressed in the thalamus with occasional expression also observed in the hippocampus, amygdala, ic, fi and cp. IL-13 expression in CD14$^{-/-}$ mice appeared to decrease at 90 dpi and was undetectable at 120 dpi. IL-13 immunoreactivity was also detected in prion-infected WT mice at 75 dpi, however, it was much less frequent than in prion-infected CD14$^{-/-}$ mice. Although IL-13 immunoreactivity was detected in the hippocampus of mock-infected WT and CD14$^{-/-}$ mice, it was weaker and occurred less frequently than in the hippocampus of prion-infected CD14$^{-/-}$ mice. Quantitative analysis showed that IL-13-positive areas in the thalamus of prion-infected CD14$^{-/-}$ mice were much larger than those of prion-infected WT mice at 75 dpi (Fig. 3B). The positive areas in prion-infected CD14$^{-/-}$ mice decreased after 90 dpi, as observed microscopically. Double immunofluorescence staining showed that IL-13-positive cells differed among the analyzed brain regions (Fig. 3E). In the thalamus, IL-13 was mostly expressed in neurons, only occasionally in microglia and rarely in astrocytes. IL-13 also appeared to be expressed in neurons in the hippocampus (data not shown). However, in the combined regions of ic, fi, and cp, IL-13 was mostly expressed in microglia, only occasionally in astrocytes, and rarely in neurons.

3.3. Expression of IL-13 receptor is upregulated in the middle stage of infection both in WT and CD14$^{-/-}$ mice

IL-13 signaling is recognized via a heterodimeric transmembrane receptor complex composed of an IL-4 receptor α (IL-4Rα) and an IL-13 receptor α1 (IL-13Rα1) [9,10]. Therefore, we assessed if IL-13Rα1 expression was also altered in the absence of CD14 (Fig. 3C). In contrast to IL-13, expression and distribution of IL-13Rα1 appeared to be similar between prion-infected WT and CD14$^{-/-}$ mice. IL-13Rα1 immunoreactivity was detected in the ic, fi, and cp at 75 dpi. IL-13Rα1-positive areas were found to spread into the corpus callosum and thalamus at 90 dpi. However, IL-13Rα1-positive cells in the corpus callosum and thalamus were almost absent at 120 dpi both in WT and CD14$^{-/-}$ mice. Quantitative analysis suggested that the IL-13α1-positive area in WT and CD14$^{-/-}$ mice at 90 dpi were similar, although variation was observed in the prion-infected CD14$^{-/-}$ mice (Fig. 3D). The cells mainly expressing IL-13Rα1 were the same as those expressing IL-13: neurons in the thalamus and microglia in the cerebral peduncle (Fig. 3F).

3.4. IL-13 expression is not completely associated with PrP^{Sc} deposition

IL-13 immunoreactivity was most frequently observed in neurons of the thalamus where PrP^{Sc} first appear in the Chandler-infected mouse brains [6]; therefore, we assessed if there was any association of PrP^{Sc} deposition with IL-13 expression. At 75 dpi, PrP^{Sc} was distributed mainly in the lateral ventral part of the thalamus in CD14$^{-/-}$ mice, the same region where IL-13 was preferentially detected (Fig. 4A). In this area, PrP^{Sc} was occasionally detected in IL-13-positive cells (Fig. 4A). Furthermore, PrP^{Sc} was detected in the same part of the thalamus in WT and CD14$^{-/-}$ mice, with its detection being more in WT mice than in CD14$^{-/-}$ mice as previously reported [6], whereas IL-13 was rarely expressed (Fig. 4B). A tendency for the concurrence of PrP^{Sc} with IL-13 expression was also observed in the hippocampus of CD14$^{-/-}$ mice (Fig. 4D). However, the presence of PrP^{Sc} did not appear to induce IL-13 in the cerebral cortex of prion-infected CD14$^{-/-}$ mice. Indeed,
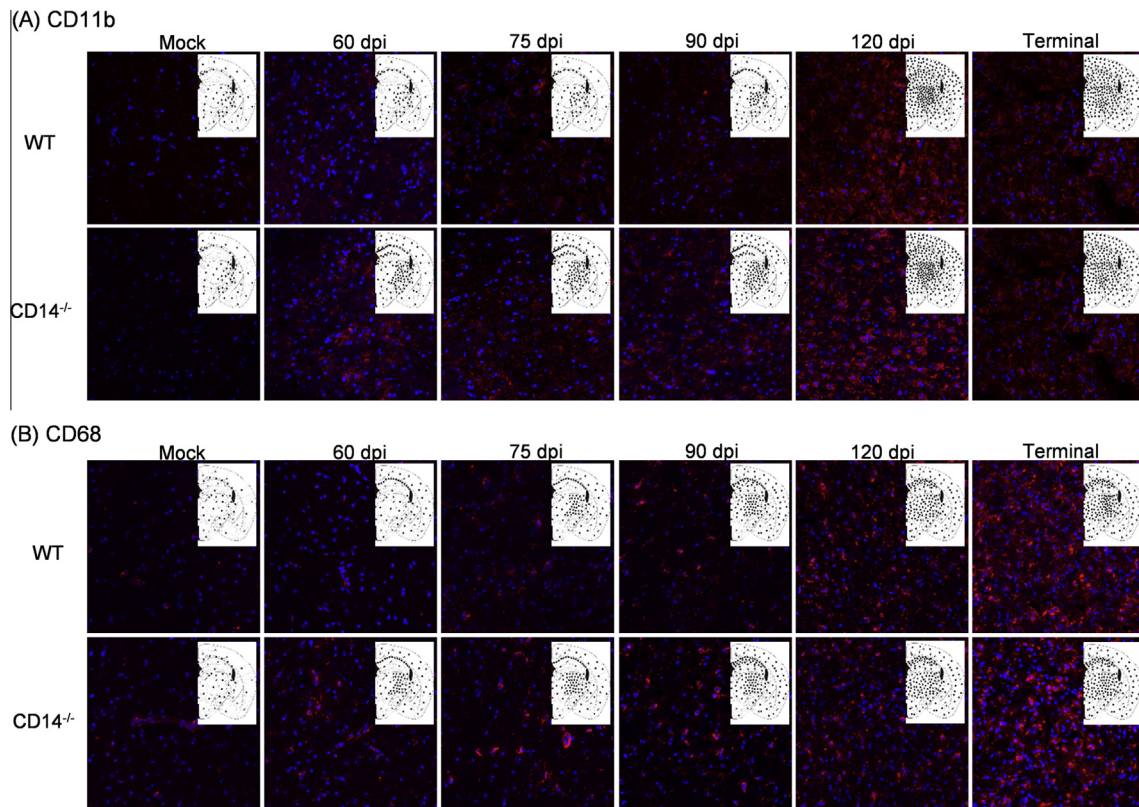
Fig. 1. Expression and distribution of microglial markers in the brains of WT and CD14$^{-/-}$ mice infected with the Chandler strain. (A) CD11b. (B) CD68. Six-week-old female WT and CD14$^{-/-}$ mice were inoculated intracerebrally with scrapie Chandler strain. For a negative control, mice were inoculated with brain homogenate prepared from uninfected WT mice. The brains were harvested at 60, 75, 90, 120 dpi and the terminal stage for frozen blocks and subjected to immune fluorescent staining. The samples were prepared from two mice for each group. Representative figures from the thalamus are shown for each time point. Figures for the mock-infected mouse brains at 60 dpi are shown as a control. Red, CD11b (A) and CD68 (B). Blue, nuclei. Bars show 50 μm. Insets show a summary of the antigen distribution, plotted as black dots on illustrations of The Mouse Brain at the level of bregma −1.82 mm [7].

IL-13 immunoreactivity was hardly detected in the cerebral cortex of CD14$^{-/-}$ mice, although the levels of PrP^{Sc} accumulated in the cerebral cortex appeared to be at least as high as those observed in the hippocampus (Fig. 4C and D).

4. Discussion

In the current study, we showed that IL-13 expression was upregulated in the absence of CD14 at the early stage of prion infection. The major cell type that expressed IL-13 in CD14$^{-/-}$ mouse brains was neurons. Considering that microglia are major cells expressing CD14 in the brain, the interaction of neurons with CD14-expressing microglia may suppress IL-13 expression in neurons. Alternatively, soluble CD14 may act as a suppressor of IL-13 expression in neurons. This theory is supported by a previous study suggesting suppression of IL-13 production from human dendritic cells by soluble CD14 molecule [11]. In the thalamus of CD14$^{-/-}$ mice at 75 dpi, IL-13 expression appeared to be concurrent with deposition of PrP^{Sc}. This observation leads us to speculate that subtle changes in neurons of the thalamus directly stimulate IL-13 expression to evoke certain protective responses. However, IL-13 expression was not induced in the cerebral cortex of prion-infected CD14$^{-/-}$ mice, suggesting that the induction of IL-13 expression cannot be simply explained by the deposition of PrP^{Sc}. Furthermore, IL-13 expression was markedly decreased after 90 dpi, whereas PrP^{Sc} deposition increased toward the terminal stage [6]. Thus, humoral factors temporarily induced in the early stage of prion infection may stimulate IL-13 expression in the brains of

CD14$^{-/-}$ mice. IL-4 is one of the factors that stimulates IL-13 expression [12]. However, gene expression of IL-4 was below the detection limit in both WT and CD14$^{-/-}$ mice (data not shown).

IL-13 was originally reported as a T cell-derived cytokine that down-regulates pro-inflammatory responses [13,14]. Although IL-13 signaling is reported to have both neuroprotective and neurotoxic effects in vivo [15–17], it has been thought to have a neuroprotective role in some neurodegenerative disorders. The levels of IL-13 in the cerebrospinal fluid of multiple sclerosis patients were related to reduced amount of Aβ, better performance in neurological test and GABAA-mediated cortical inhibition [18]. Intracerebral microinjections of IL-4 and IL-13 reduced Aβ accumulation in APP23 mice and promoted phagocytosis and the increased expression of neprilysin in neurons, which leads to degradation of Aβ [19]. A previous study showed that the survival time of IL-13 deficient mice was shortened compared with WT mice following intracerebral inoculation with a low dose of Chandler strain; however, no difference was observed with a high dose inoculation [20]. Low IL-13 expression in prion-infected WT mouse brains, as shown in the current study, may be one of the reasons why the IL-13 knockout had a limited effect on the survival time. Nevertheless, the increased prion susceptibility of IL-13$^{-/-}$ mice indicates the possible involvement of IL-13 in the pathogenesis of prion diseases.

This study, along with our previous work, has shown that CD14 deficiency evokes temporal anti-inflammatory condition in the brain in the early and middle stage of prion infection. It is of interest to clarify whether anti-inflammatory responses reduce the production of pro-inflammatory cytokines. In the previous study, IL-
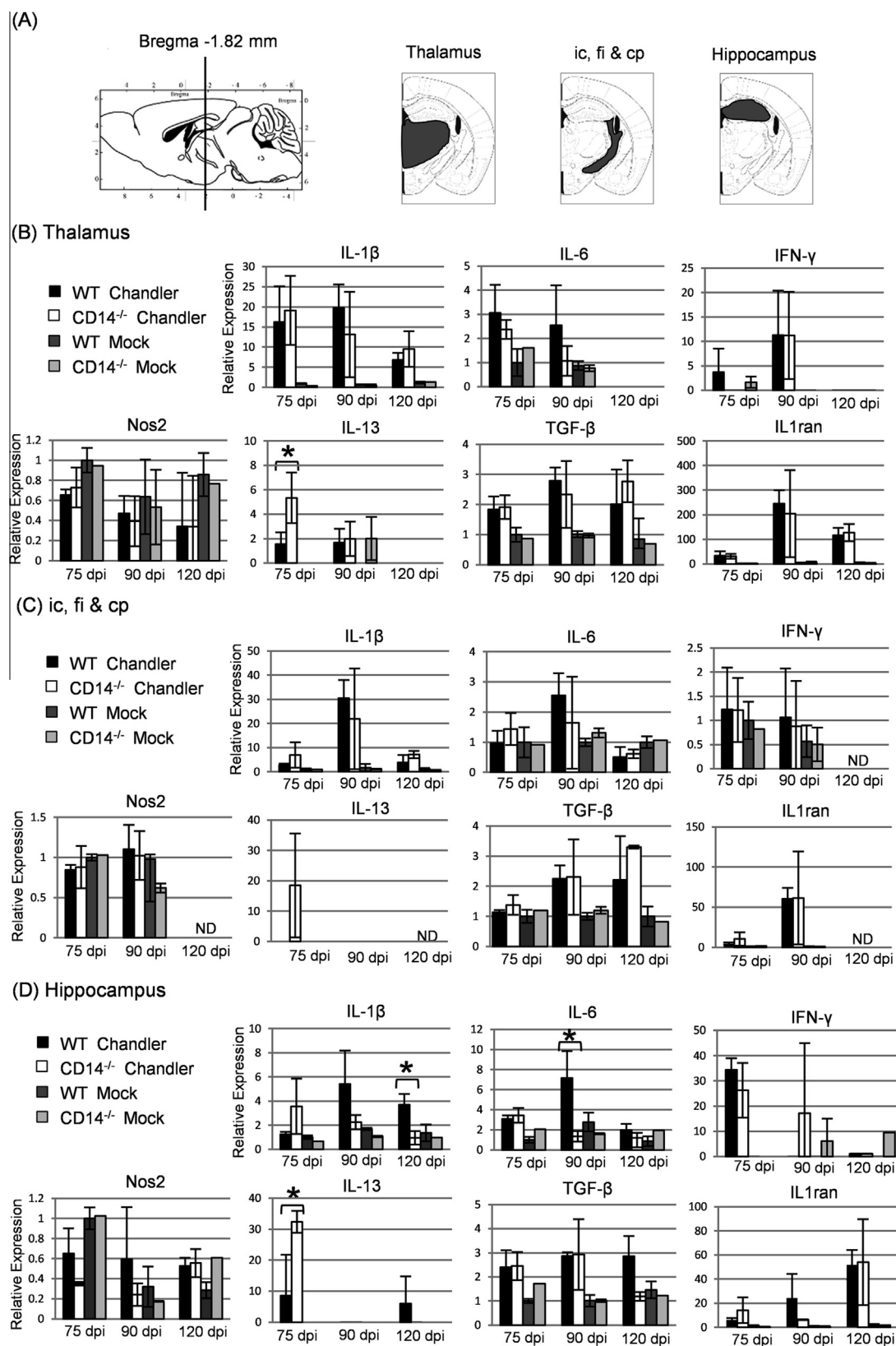
Fig. 2. Cytokine gene expression in the brains of WT and CD14$^{-/-}$ mice infected with prion. (A) Regions subjected to the analysis: thalamus, hippocampus, and combined regions of ic, fi and cp. Total RNA was extracted from each region at 75, 90, and 120 dpi and subjected to quantitative RT-PCR. (B–D) Relative expression of cytokine genes in the thalamus (B), the region of ic, fi and cp (C) and the hippocampus (D). Expression level of the corresponding gene of the mock-infected mice at 75 dpi was defined as 1. When gene expression in the mock-infected WT mice was below the detection limit, expression level at 40 cycles was tentatively defined as 1 for the calculation of relative fold changes. Graphs show the mean with standard deviations ($n = 3$), except for mock-infected CD14$^{-/-}$ mice at 75 and 120 dpi ($n = 2$). $^*p < 0.05$, student's t-test. ND: not determined.
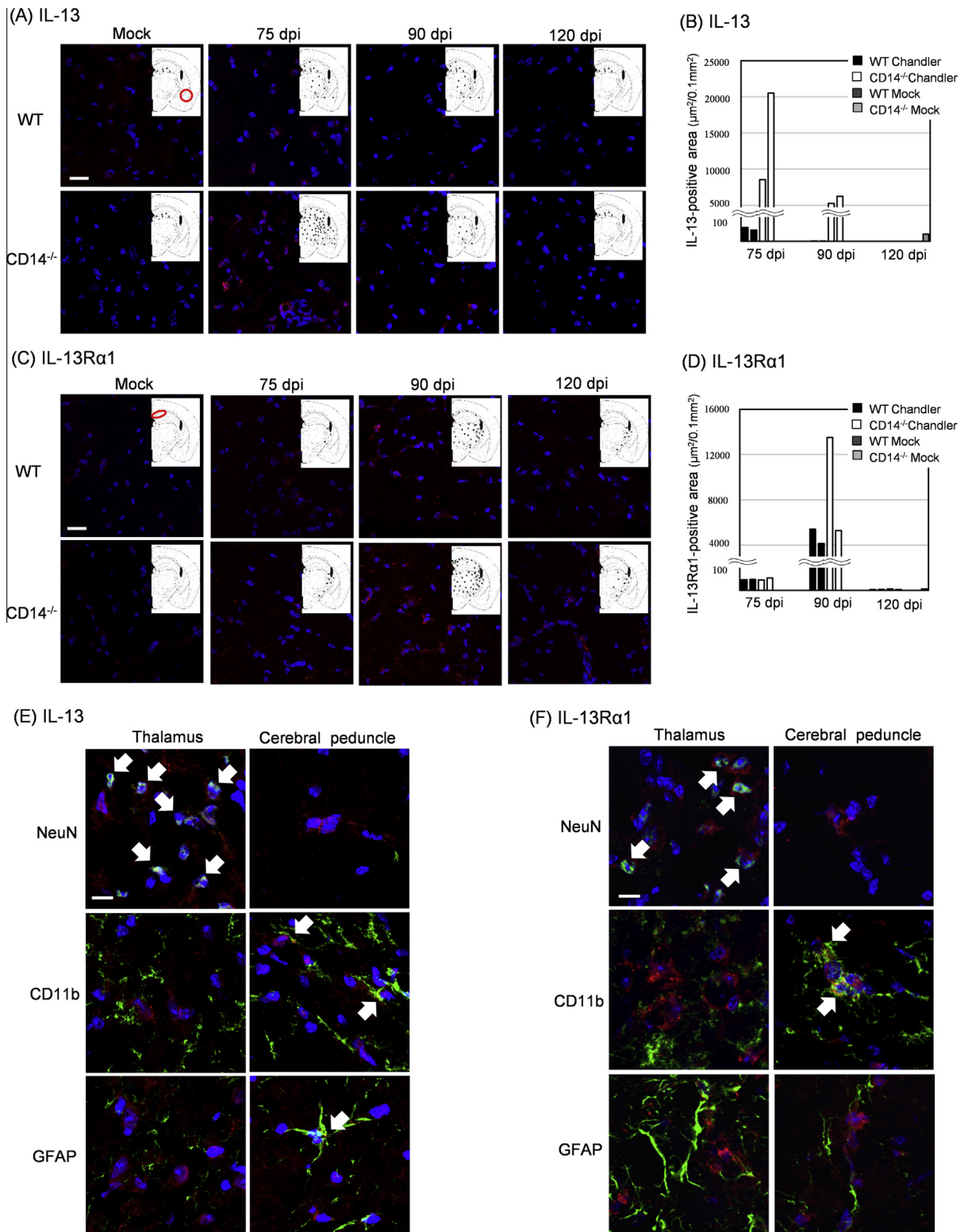
Fig. 3. Expression and distribution of IL-13 and IL-13Rα1 in the brains of WT and CD14$^{-/-}$ mice infected with prion. (A and C) Expression and distribution of IL-13 (A) and IL-13 Rα1 (C) at 75, 90, and 120 dpi. Frozen sections at the level of bregma −1.82 mm were subjected to immunofluorescence staining using rabbit polyclonal antibodies against IL-13 and IL-13Rα1. Representative figures from the thalamus are shown. Red, IL-13 or IL-13Rα1. Blue, nuclei. Bars, 20 μm. The insets show a summary of the distribution, plotted as black dots on illustrations of The Mouse Brain at the bregma −1.82 mm [7]. The amygdala and corpus callosum are circled on the insets in (A) and (C), respectively. (B and D) Quantitative results. Graphs show the quantification of positive areas for IL-13 (B) and IL-13Rα1 (D), measured by Imaris ver 7.6.1. The number of examined mice was two, except for the mock-infected CD14$^{-/-}$ mouse at 90 and 120 dpi (n = 1). (E and F) Double immunofluorescence staining of IL-13 (E) at 75 dpi or IL-13 Rα1 (F) at 90 dpi with neuronal and glial cell markers in the thalamus and the cerebral peduncle. Green: NeuN (neurons), CD11b (microglia) or GFAP (astrocytes). Red: IL-13 or IL-13 Rα1. Blue: nuclei. Bars, 10 μm. Arrows, double-positive cells for IL-13 or IL-13Rα1 with any of the markers.
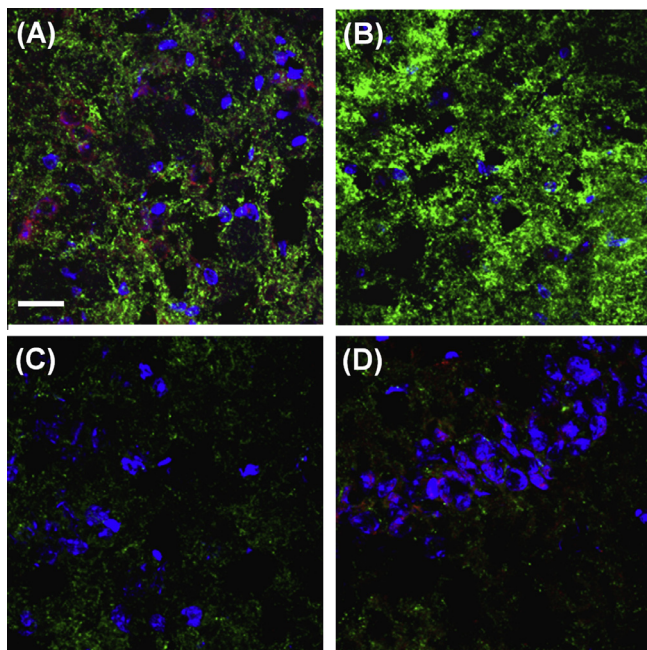
Fig. 4. Distributions of PrP^{Sc} and IL-13 in Chandler-infected WT and CD14$^{-/-}$ mouse brains. Frozen sections at 75 dpi were used. Because GdnSCN treatment for the PrP^{Sc}-specific detection weakened the IL-13 immunoreactivity, sections were first subjected to staining for IL-13. After the fixation with 4% paraformaldehyde for 10 min, sections were treated with 5 M GdnSCN for 10 min and PrP^{Sc}-specific immunofluorescence staining was performed [6,21]. (A) Thalamus of CD14$^{-/-}$ mouse. (B) Thalamus of WT mouse. (C) Cerebral cortex of CD14$^{-/-}$ mouse. (D) Hippocampus of CD14$^{-/-}$ mouse. Green, PrP^{Sc}. Red, IL-13. Blue, nuclei. Bars, 20 μm.

1β-positive area in the internal capsule of prion-infected CD14$^{-/-}$ mice was smaller than that of prion-infected WT mice at 60 dpi [6]. However, gene expressions of pro-inflammatory cytokines at 75 dpi did not show this tendency (Fig. 2), although lower expressions of IL-1β and IL-6 in CD14$^{-/-}$ mice were occasionally observed in the hippocampus (Fig. 2D). The apparent discrepancy in the gene and protein expression of IL-1β in the current and previous study may be due to a difference of the sampling area: 10 μm-thickness for immunofluorescence staining and approximately 1 mm-thickness for gene expression analysis, which is the limitation of thin-slice using the Alto™ Brain Matrix. Thus, any difference in the IL-1β expression observed by immunofluorescence staining might be overwhelmed by collecting tissue from a larger area.

The mechanism for the temporal upregulation of anti-inflammatory cytokines in prion-infected CD14$^{-/-}$ mice remains to be elucidated. However, temporal induction of anti-inflammatory milieu slows disease progression by interfering with prion propagation. This indicates that immunomodulation that evokes long-lasting anti-inflammatory responses may be a candidate for therapeutics of prion diseases.

Acknowledgments

References

[1] B.M. Bradford, N.A. Mabbott, Prion disease and the innate immune system, Viruses-Basel 4 (2012) 3389–3419.
[2] E.A. Frey, D.S. Miller, T.G. Jahr, A. Sundan, V. Bazil, T. Espevik, B.B. Finlay, S.D. Wright, Soluble CD14 participates in the response of cells to lipopolysaccharide, J. Exp. Med. 176 (1992) 1665–1671.
[3] S.D. Wright, R.A. Ramos, P.S. Tobias, R.J. Ulevitch, J.C. Mathison, CD14, a receptor for complexes of lipopolysaccharide (LPS) and LPS binding protein, Science 249 (1990) 1431–1433.
[4] J.C. Chow, D.W. Young, D.T. Golenbock, W.J. Christ, F. Gusovsky, Toll-like receptor-4 mediates lipopolysaccharide-induced signal transduction, J. Biol. Chem. 274 (1999) 10689–10692.
[5] C.J. Kirschning, H. Wesche, T. Merrill Ayres, M. Rothe, Human toll-like receptor 2 confers responsiveness to bacterial lipopolysaccharide, J. Exp. Med. 188 (1998) 2091–2097.
[6] K. Sakai, R. Hasebe, Y. Takahashi, C.H. Song, A. Suzuki, T. Yamasaki, M. Horiuchi, Absence of CD14 delays progression of prion diseases accompanied by increased microglial activation, J. Virol. 87 (2013) 13433–13445.
[7] G. Paxinos, K.B.J. Franklin, The Mouse Brain in Stereotaxic Coordinates, second ed., Academic Press, San Diego, 2001.
[8] C.L. Kim, A. Umetani, T. Matsui, N. Ishiguro, M. Shinagawa, M. Horiuchi, Antigenic characterization of an abnormal isoform of prion protein using a new diverse panel of monoclonal antibodies, Virology 320 (2004) 40–51.
[9] D. Caput, P. Laurent, M. Kaghad, J.M. Lelias, S. Lefort, N. Vita, P. Ferrara, Cloning and characterization of a specific interleukin (IL)-13 binding protein structurally related to the IL-5 receptor alpha chain, J. Biol. Chem. 271 (1996) 16921–16926.
[10] S.M. Zurawski, F. Vega Jr., B. Huyghe, G. Zurawski, Receptors for interleukin-13 and interleukin-4 are complex and share a novel component that functions in signal transduction, EMBO J. 12 (1993) 2663–2670.
[11] A.C. Lundell, K. Andersson, E. Josefsson, A. Steinkasserer, A. Rudin, Soluble CD14 and CD83 from human neonatal antigen-presenting cells are inducible by commensal bacteria and suppress allergen-induced human neonatal Th2 differentiation, Infect. Immun. 75 (2007) 4097–4104.
[12] T. Jung, J. Wijdenes, C. Neumann, J.E. de Vries, H. Yssel, Interleukin-13 is produced by activated human CD45RA+ and CD45RO+ T cells: modulation by interleukin-4 and interleukin-12, Eur. J. Immunol. 26 (1996) 571–577.
[13] A.N.J. Mckenzie, J.A. Culpepper, R.D. Malefyt, F. Briere, J. Punnonen, G. Aversa, A. Sato, W. Dang, B.G. Cocks, S. Menon, J.E. Devries, J. Banchereau, G. Zurawski, Interleukin-13, a T-cell-derived cytokine that regulates human monocyte and B-cell function, Proc. Natl. Acad. Sci. U.S.A. 90 (1993) 3735–3739.
[14] A. Minty, P. Chalon, J.M. Derocq, X. Dumont, J.C. Guillemot, M. Kaghad, C. Labit, P. Leplatois, P. Liauzun, B. Miloux, C. Minty, P. Casellas, G. Loison, J. Lupker, D. Shire, P. Ferrara, D. Caput, Interleukin-13 is a new human lymphokine regulating inflammatory and immune-responses, Nature 362 (1993) 248–250.
[15] B.E. Morrison, M.C. Marcondes, D.K. Nomura, M. Sanchez-Alavez, A. Sanchez-Gonzalez, I. Saar, K.S. Kim, T. Bartfai, P. Maher, S. Sugama, B. Conti, Cutting edge: IL-13Ralpha1 expression in dopaminergic neurons contributes to their oxidative stress-mediated loss following chronic peripheral treatment with lipopolysaccharide, J. Immunol. 189 (2012) 5498–5502.
[16] K.W. Park, H.H. Baik, B.K. Jin, IL-13-induced oxidative stress via microglial NADPH oxidase contributes to death of hippocampal neurons in vivo, J. Immunol. 183 (2009) 4666–4674.
[17] W.H. Shin, D.Y. Lee, K.W. Park, S.U. Kim, M.S. Yang, E.H. Joe, B.K. Jin, Microglia expressing interleukin-13 undergo cell death and contribute to neuronal survival in vivo, Glia 46 (2004) 142–152.
[18] S. Rossi, R. Mancino, A. Bergami, F. Mori, M. Castelli, V. De Chiara, V. Studer, G. Mataluni, G. Sancesario, V. Parisi, H. Kusayanagi, G. Bernardi, C. Nucci, S. Bernardini, G. Martino, R. Furlan, D. Centonze, Potential role of IL-13 in neuroprotection and cortical excitability regulation in multiple sclerosis, Multiple Sclerosis J. 17 (2011) 1301–1312.
[19] K. Kawahara, M. Suenobu, A. Yoshida, K. Koga, A. Hyodo, H. Ohtsuka, A. Kuniyasu, N. Tamamaki, Y. Sugimoto, H. Nakayama, Intracerebral microinjection of interleukin-4/interleukin-13 reduces beta-amyloid accumulation in the ipsilateral side and improves cognitive deficits in young amyloid precursor protein 23 mice, Neuroscience 207 (2012) 243–260.
[20] A.M. Thackray, A.N. McKenzie, M.A. Klein, A. Lauder, R. Bujdoso, Accelerated prion disease in the absence of interleukin-10, J. Virol. 78 (2004) 13697–13707.
[21] T. Yamasaki, A. Suzuki, T. Shimizu, M. Watarai, R. Hasebe, M. Horiuchi, Characterization of intracellular localization of PrP(Sc) in prion-infected cells using a mAb that recognizes the region consisting of aa 119–127 of mouse PrP, J. Gen. Virol. 93 (2012) 668–680.